7600 *Biochemistry* **2010,** *49,* 7600–7614
DOI: 10.1021/bi100599b

BIOCHEMISTRY
including biophysical chemistry & molecular biology
Article

S-Adenosyl-L-methionine Regulation of the Cardiac Ryanodine Receptor Involves Multiple Mechanisms[†]

Angela J. Kampfer and Edward M. Balog*

School of Applied Physiology, Georgia Institute of Technology, Atlanta, Georgia 30332

Received April 19, 2010; Revised Manuscript Received July 12, 2010

ABSTRACT: Cardiac contraction is triggered by the release of Ca^{2+} via the ryanodine receptor (RyR2), a sarcoplasmic reticulum (SR) resident ion channel. RyR2 channel activity is modulated through ligand binding and posttranslational regulatory mechanisms. *S*-Adenosyl-L-methionine (SAM), the primary methyl group donor for enzyme-mediated methylation of proteins and other biological targets, activates RyR2 via an unknown mechanism. Here we show that the SAM-induced increase in cardiac SR (CSR) vesicle [^{3}H]ryanodine binding is unaffected by methyltransferase inhibitors and immunoprecipitation of RyR2 from *S*-adenosyl-L-[*methyl*-^{3}H]methionine ([^{3}H]SAM) pretreated CSR indicates that RyR2 is not a target of SAM-mediated protein methylation. Because SAM contains an adenosine moiety and RyR2 is activated by ATP, we investigated whether SAM exerts its effects through the adenine nucleotide binding sites on the RyR2 channel. In support of this hypothesis, the SAM and ATP concentration dependence of CSR vesicle [^{3}H]ryanodine binding virtually overlaps. Furthermore, ryanodine binding assays show that SAM competes with adenine nucleotide activation of RyR2, and the effects of SAM on mean channel open and closed times follow similar trends as those observed for ATP. Interestingly, SAM but not ATP activation of RyR2 was associated with a marked increase in the percent of channel openings to a subconductance level ~60% of the maximal single channel conductance. This work highlights the complexity underlying SAM regulation of RyR2 and suggests ligand binding is among the multiple mechanisms responsible for SAM regulation of RyR2.

The ryanodine receptor (RyR)[1] is an intracellular Ca^{2+} channel located in the sarcoplasmic reticulum (SR) membrane which serves as a gated efflux pathway for stored Ca^{2+}. Mobilization of intracellular Ca^{2+} via the cardiac isoform of the channel (RyR2) is the event which triggers contraction; thus, RyR2 plays a critical role in the contractile performance of the heart. RyRs are high molecular weight homotetramers consisting of a C-terminal SR membrane spanning domain and a large N-terminal cytoplasmic domain (*1*). Each RyR tetramer exists in its native membrane as part of a macromolecular complex in association with a number of signaling molecules involved in posttranslational protein modification. The RyR is also subject to complex allosteric regulation by metabolites, ions, and pharmacological agents (*2*). Physiological RyR regulatory ligands include Ca^{2+}, Mg^{2+}, ATP, and the accessory proteins calmodulin (CaM) and FK506 binding proteins (FKBPs).

ATP activates RyR2 in a concentration and Ca^{2+}-dependent manner (*3*) and is present in resting muscle at a concentration sufficiently high for it to function as a principal cellular regulator of RyR2 (*4*). Although the degree to which adenine nucleotides (e.g., ATP and its metabolites) activate RyR2 varies, all are thought to interact with the same class of binding sites on the channel. The purine ring is important for agonist activity at these sites, as the replacement of adenine with guanine destroys the ability of the nucleotide to modulate RyR (*3*). However, other structural features that determine the ability of adenosine-based compounds to activate RyR2 are poorly defined.

The biological methyl group donor *S*-adenosyl-L-methionine (SAM) participates in transmethylation reactions whereby the methyl group of SAM is transferred to proteins, nucleic acids, or lipids, thereby altering the localization and/or function of the methylated target (*5*−*7*). Previous reports of a SAM-induced enhancement of cardiac contraction did not investigate the effects of SAM on RyR2 (*8*, *9*). More recently, Chen et al. (*10*) attributed SAM activation of RyRs from coronary artery myocytes to protein methylation causing the dissociation of the RyR accessory protein FKBP12. However, smooth muscle expresses RyR1, RyR2 (*11*, *12*), and RyR3 (*13*); therefore, the effects of SAM on RyRs from artery myocytes reflect SAM acting on multiple channel isoforms (*10*).

In contrast to the effects of SAM observed by Chen and colleagues (*10*), our prior work suggests SAM activates RyR2 through a direct interaction with the channel (*14*). Importantly, SAM is an adenosine-based compound which raises the possibility that SAM, like ATP, regulates RyR2 via the adenine nucleotide binding site(s). In the present study we have examined the effects of SAM on a defined RyR isoform by utilizing cardiac SR (CSR) vesicle ryanodine binding and current recordings from native RyR2 channels incorporated into phospholipid bilayers. Our primary aim was to clarify how SAM exerts its effect on RyR2 activity, specifically, whether SAM acts via a direct (e.g., ligand binding) or an indirect (e.g., posttranslational modification) mechanism. In addition to the previously reported activation of

[†]This work was supported by an AHA Southeast Affiliate Predoctoral Fellowship to A.J.K. and an AHA Scientist Development Grant to E.M.B.

*To whom correspondence should be addressed. Phone: 404- 894-3957. Fax: 404-894-9982. E-mail: ed.balog@ap.gatech.edu.

[1]Abbreviations: RyR2, cardiac ryanodine receptor; SR, sarcoplasmic reticulum; CSR, cardiac SR; SAM, *S*-adenosyl-L-methionine; SAH, *S*-adenosyl-L-homocysteine; CaM, calmodulin; FKBP, FK506 binding protein; SERCA, sarcoplasmic/endoplasmic reticulum calcium ATPase.

 Published on Web 08/02/2010

RyR2 by SAM, we observe a distinct SAM-induced channel subconductance state. Our data indicate that SAM binding the RyR2 adenine nucleotide site(s) results in channel activation while a distinct mechanism underlies the effect of SAM on RyR2 conductance.

MATERIALS AND METHODS

Materials. Pigs were purchased from Clemson University Research Farm Services. Unlabeled ryanodine and 3-[(3-cholamidopropyl)dimethylammonio]-1-propanesulfonate (CHAPS) were obtained from Calbiochem (La Jolla, CA). Adenosine 5′-(β,γ-imido)triphosphate tetralithium salt (AMPPNP), *S*-(5′-adenosyl)-L-methionine chloride (SAM), *S*-(5′-adenosyl)-L-homocysteine (SAH), sinefungin, FK506, ATP, and ADP were obtained from Sigma (St. Louis, MO). [^{3}H]Ryanodine and *S*-adenosyl-L-[*methyl*-^{3}H]methionine ([^{3}H]SAM) were obtained from Perkin-Elmer (Waltham, MA). FKBP12.6 antibodies were obtained from R&D Systems (no. AF4174; Minneapolis, MN). RyR2 monoclonal antibody (clone C3-33) was from Sigma-Aldrich (St. Louis, MO). Horseradish preoxidase conjugated antibodies donkey anti-goat and goat anti-mouse were obtained from Santa Cruz Biotechnology (Santa Cruz, CA) and Millipore (Billerica, MA), respectively. EcoLite scintillation fluid and protease inhibitors were purchased from MP Biomedicals (Solon, OH). The ECL Plus Western blotting detection system was from GE Healthcare. Bio-Max light film was obtained from Kodak. Whatman GF/B filters were from Brandel, Inc. (Gaithersberg, MD), and BioTrace PVDF membranes were from Life Sciences (Pensacola, FL). Recombinant protein G−Sepharose 4B beads were obtained from Invitrogen (Carlsbad, CA). Phospholipids were purchased from Avanti Polar Lipids (Alabaster, AL).

Isolation of Cardiac Sarcoplasmic Reticulum Vesicles. Cardiac SR (CSR) vesicles used for [^{3}H]ryanodine binding were prepared from porcine ventricular tissue as previously described (*15*). Animals were euthanized in accordance with the Public Health Services Policy on Humane Care and Use of Laboratory Animals and with the approval of the Institutional Care and Use Committee of the Georgia Institute of Technology. Briefly, animals were euthanized by intravenous injection of sodium pentobarbital (100 mg/kg) following sedation by subcutaneous injection of ketamine (20 mg/kg) and xylazine (2 mg/kg). Muscle was homogenized in ice-cold 10 mM $NaHCO_3$ buffer, and the supernatant from a 4000*g* centrifugation was filtered through cheesecloth, recentrifuged, and retained. Membranes pelleted at 80000*g* from the supernatant were extracted in 0.6 M KCl and 20 mM Tris (pH 6.8), centrifuged at 120000*g*, and resuspended in a minimal volume of 10% sucrose. Heavy CSR vesicles isolated based on the method of Sitsapesan and Williams (*16*) were used for channel recordings as they incorporated more readily into phospholipid bilayers. Muscle was homogenized in a buffer containing 300 mM sucrose and 20 mM piperazine-*N*,*N*′-bis(2-ethanesulfonic acid) (PIPES) (pH 7.4) and centrifuged at 10000*g*, and the retained supernatant was centrifuged a second time at 87000*g*. The pelleted membranes were resuspended in a salt solution (400 mM KCl, 0.5 mM $MgCl_2$, 0.5 mM $CaCl_2$, 0.5 mM EGTA, 25 mM PIPES, pH 7.0) containing 10% sucrose (w/v). The mixed membrane suspension was layered upon discontinuous sucrose density gradients consisting of identical salt solutions containing 20%, 30%, and 40% sucrose (w/v) and sedimented at 100000*g*. Heavy CSR membrane vesicles collected at the 30−40% sucrose interface were diluted in 400 mM KCl, pelleted at 87000*g*, and resuspended in a minimal volume of buffer containing 400 mM sucrose and 5 mM 4-(2-hydroxyethyl)-1-piperazineethanesulfonic acid (HEPES) (pH 7.2). All isolation buffers contained a mixture of protease inhibitors (aprotinin, leupeptin, pepstatin A, benzamidine, and phenylmethanesulfonyl fluoride). Vesicles were frozen rapidly in liquid N_2 and stored at −80 °C.

[^{3}H]SAM/SAM Pretreatment of CSR Vesicles and Determination of [^{3}H]Methyl Incorporation. CSR vesicles (4 mg/mL) were incubated in media containing 20 mM PIPES (pH 7.0), 150 mM KCl, and 0.285 μM (3 μCi) *S*-adenosyl-L-[*methyl*-^{3}H]methionine ([^{3}H]SAM) ± 1 mM *S*-adenosyl-L-homocysteine (SAH) and/or 500-fold excess of unlabeled SAM for 30 min at 37 °C. In a subset of experiments CSR was incubated as described above but in the presence of 0.1 or 2 mM unlabeled SAM rather than [^{3}H]SAM. Treated CSR vesicles were pelleted by centrifugation through 15% sucrose. Pellets were washed by resuspension in 10% sucrose followed by centrifugation at 100000*g*. Washed CSR vesicles were resuspended in a minimal volume of 10% sucrose, flash frozen in liquid N_2, and stored at −80 °C. SAM-treated heavy CSR used for channel recording experiments was resuspended in a minimal volume of buffer containing 400 mM sucrose and 5 mM HEPES (pH 7.2). All buffers contained a mixture of protease inhibitors. For determining [^{3}H]methyl incorporation, an aliquot of treated CSR vesicles (100 μg) was collected by filtration onto Whatman GF/B filters and washed with 8 mL of ice-cold 100 mM KCl, and the activity retained was measured by liquid scintillation counting.

RyR2 Immunoprecipitation and Determination of [^{3}H]-Methyl Incorporation. Control or [^{3}H]SAM-pretreated CSR vesicles (200 μg) were solubilized overnight at 4 °C in buffer containing 3% CHAPS, 1.0 M NaCl, 20 mM Tris-HCl (pH 7.4), 1 mM dithiothreitol, and protease inhibitors and centrifuged at 12000*g* for 10 min. Solubilized CSR was incubated for 2 h at 4 °C with or without a RyR2 specific antibody (1:100) with rotary mixing and for an additional 2 h followed by the addition of protein G−Sepharose CL-4B beads (20 μL). Beads were pelleted by centrifugation at 14000*g* and washed twice with IP buffer containing 20 mM Tris-HCl (pH 7.4), 1.0 M NaCl, 0.4% CHAPS, and protease inhibitors. Proteins were eluted from the affinity beads by boiling in sample buffer containing 10% sodium dodecyl sulfate (SDS). For determining [^{3}H]methyl incorporation into immunoprecipitated samples, radioactivity of an aliquot (20 μL) of eluted proteins was determined by liquid scintillation counting.

FK506 Treatment of CSR Vesicles. Treatment of CSR vesicles was based on the method of Ahern et al. for the removal of FKBP12 from RyRs (*17*). CSR vesicles (2 mg/mL) were incubated at 37 °C for 30 min in media containing 20 mM imidazole (pH 7.4), 300 mM sucrose, protease inhibitors, and 10 μM FK506 (in ethanol) or an equivalent volume of ethanol as control. Vesicles were pelleted at 24000*g*, washed in buffer, and repelleted before resuspension in a minimal volume of buffer.

Western Blotting. CSR vesicles and immunoprecipitated RyR2 samples were separated on 5% or 5−20% gradient SDS−polyacrylamide gels using the buffer system of Laemmli (*18*) and transferred to PVDF membranes for 18 h at 30 V followed by 60 min at 200 V with current limited to 0.5 A using a buffer of 25 mM Tris, pH 8.3, 192 mM glycine, 20% methanol, and 0.05% SDS at 4 °C. After blocking for 1 h at room temperature in fresh 5% BSA in PBS containing 0.1% Tween-20 (PBS-T), membranes were exposed to FKBP12.6 antibodies diluted to 1:1000 in PBS-T,

5% BSA, and 0.5 M NaCl overnight at 4 °C. After washing and incubating in horseradish peroxidase conjugated donkey anti-goat IgG (1:100000) for 1 h at room temperature, reacted bands were visualized using enhanced chemiluminescence. Antibody complexes were stripped from the membrane by incubation in 100 mM 2-mercaptoethanol, 2% SDS, and 62.5 mM tris-(hydroxymethyl)aminomethane, pH 6.7, at 50 °C for 30 min. RyR2 was detected either after transfer of proteins to PDVF membranes or after stripping membranes previously probed for FKBP12.6. RyR2 monoclonal C3-33 was used at a dilution of 1:50000. The secondary horseradish peroxidase conjugated goat anti-mouse antibody was used at a dilution of 1:20000.

[^{3}H]Ryanodine Binding. [^{3}H]Ryanodine binding measurements are sensitive indicators of RyR2 channel activity as ryanodine binds with high affinity and selectively to RyRs in the open state (*19*, *20*). Ryanodine binding buffer contained 0.4 mg/mL CSR vesicles, 7 nM [^{3}H]ryanodine, 150 mM KCl, 20 mM K-PIPES (pH 7.0), 0.1 mg/mL BSA, 1.0 μg/mL leupeptin, 1.0 μg/mL aprotinin, and Ca^{2+}−EGTA buffers to achieve the desired free Ca^{2+} concentrations (*21*). Estimates of maximal [^{3}H]ryanodine binding capacity of CSR vesicle preparations were made in parallel with each experiment in media that in addition contained 500 mM KCl, 5 mM ATP, 100 μM Ca^{2+}, and 50 nM ryanodine. Nonspecific CSR vesicle [^{3}H]ryanodine binding was determined by inclusion of 10 mM $MgCl_2$ and 20 μM unlabeled ryanodine in the binding media. After 20 h at room temperature (20−22 °C) CSR vesicles were collected on Whatman GF/B filters and washed with 8 mL of ice-cold 100 mM KCl. Radioactivity retained by the filters was determined by liquid scintillation counting.

The Ca^{2+} dependence of ryanodine binding data was fit with eq 1:

$$[^3\text{H}]\text{ryanodine bound} = B'\left(\frac{[Ca^{2+}]}{[Ca^{2+}]^{n_a} + EC_{50}{}^{n_a}}\right)\left(1 - \frac{[Ca^{2+}]}{[Ca^{2+}]^{n_i} + IC_{50}{}^{n_i}}\right) \quad (1)$$

where B' is the maximal [^{3}H]ryanodine binding in the presence of a specific concentration of ligand. This differs from maximal CSR vesicle [^{3}H]ryanodine binding (B_{max}) determined via saturation analysis, which refers to the amount of ryanodine bound in the presence of an infinite concentration of ligand. The EC_{50} and IC_{50} are the Ca^{2+} concentrations required to half-maximally activate and inhibit [^{3}H]ryanodine binding, respectively, and n_a and n_i are Hill coefficients for activation and inhibition, respectively. The effects of SAM on B_{max} and ryanodine dissociation constant (K_d) were determined by saturation analysis using nonlinear curve fitting of eq 2 to binding isotherms.

$$[^3\text{H}]\text{ryanodine bound} = B_{max}X[\text{ryanodine}]/(K_d + [\text{ryanodine}]) \quad (2)$$

All curve fitting was performed using SigmaPlot 9.0 (Systat Software, Point Richmond, CA). All assays were performed in duplicate and were repeated using at least four different CSR vesicle preparations.

Single Channel Recordings. Muller−Rudin bilayers were formed by painting a lipid mixture (phosphatidylethanolamine, phosphatidylserine, phosphatidylcholine, 5:3:2 ratio by wt, 50 mg/mL dissolved in *n*-decane) across a 100−250 μm aperture in a Delrin cup. To assist in vesicle fusion, an osmotic gradient was established across the bilayer. Heavy CSR vesicles were added to the *cis* chamber which contained 250 mM cesium methanesulfonate, 10 mM HEPES (pH 7.4), and 1 mM $CaCl_2$. The *trans* chamber contained 50 mM cesium methansulfonate and 10 mM HEPES, pH 7.4. After incorporation of channels into the bilayer, the concentration of cesium methansulfonate in the *trans* chamber was raised to 250 mM and the *cis* chamber Ca^{2+} concentration adjusted by adding small aliquots of concentrated EGTA and $CaCl_2$ (*21*). Small aliquots of concentrated channel regulators were added to the *cis* chamber with stirring prior to data acquisition. Voltage was controlled, and channel currents were recorded using an Axoclamp 200B patch clamp amplifier (Molecular Devices). The *cis* and *trans* chambers were connected to the amplifier head stage by Ag/AgCl electrodes and agar salt bridges. The *trans* chamber was held at ground, and current was applied to the *cis* chamber. Current was monitored on an oscilloscope, filtered at 1 kHz, and recorded at 5 kHz. Channel data were collected using a pulsing protocol in which the potential was held at 0 mV for 120 ms between steps of 4 s duration to −70 mV (CLAMPEX program, pCLAMP software, Axon instruments).

Analysis of Data. Only channels having a conductance of at least 400 pS were used for analysis. Single-channel current amplitudes were measured from digitized data using manually controlled cursors. Channel open probability (P_o), open times, and closed times were determined by the half-amplitude threshold method with a threshold set so that openings to the maximum single channel conductance level (γ_{max}) and openings to the SAM-related subconductance level ~20 pA (γ_{sub}) were included in the analyses. Single channel P_o was calculated from at least 30 4 s sweeps using pCLAMP9.2 (Molecular Devices). Frequently, two channels incorporated into the bilayer, indicated by current amplitudes of twice the expected magnitude, and P_o was estimated as the average P_o of the two channels, calculated as [P_o level 1 + (P_o level 2 × 2)]/2. Bilayers in which three or four channels had incorporated were treated similarly. The probability of openings to γ_{sub} (P_o substate) was calculated as time spent in γ_{sub}/total recording time. The percentage of channel openings to subconductance levels was given by [P_o substate/(P_o substate + P_o maximum single channel conductance level (≥20 pA)) × 100].

Statistics. CSR [^{3}H]ryanodine binding and [^{3}H]methyl group incorporation data are presented as means ± SEM and were analyzed using a one-way ANOVA with a Holm−Sidak multiple comparison as a posthoc test or by Student's *t* tests as appropriate. Occasionally data did not fit the assumptions required for a *t* test, in which case a nonparametric test was performed. Single channel open probabilities and dwell times are presented as means ± SEM and were analyzed using Student's paired *t* tests or Mann−Whitney rank sum test. Statistical analysis was performed using SigmaStat 3.1 (Systat Software, Point Richmond, CA). The level of significance was $p < 0.05$ unless otherwise noted.

RESULTS

Effects of SAM on CSR Vesicle [^{3}H]Ryanodine Binding. *S*-Adenosyl-L-methionine (SAM) is a ubiquitous methyl group donor which is present in cells at a concentration of 60−90 μM (*5*, *22*). Previously we have shown that SAM (≥75 μM) significantly increases CSR vesicle [^{3}H]ryanodine binding in a concentration-dependent manner (*14*). Thus, RyR2 is activated by a physiological concentration of SAM. The effects of SAM on the Ca^{2+} concentration dependence of CSR vesicle

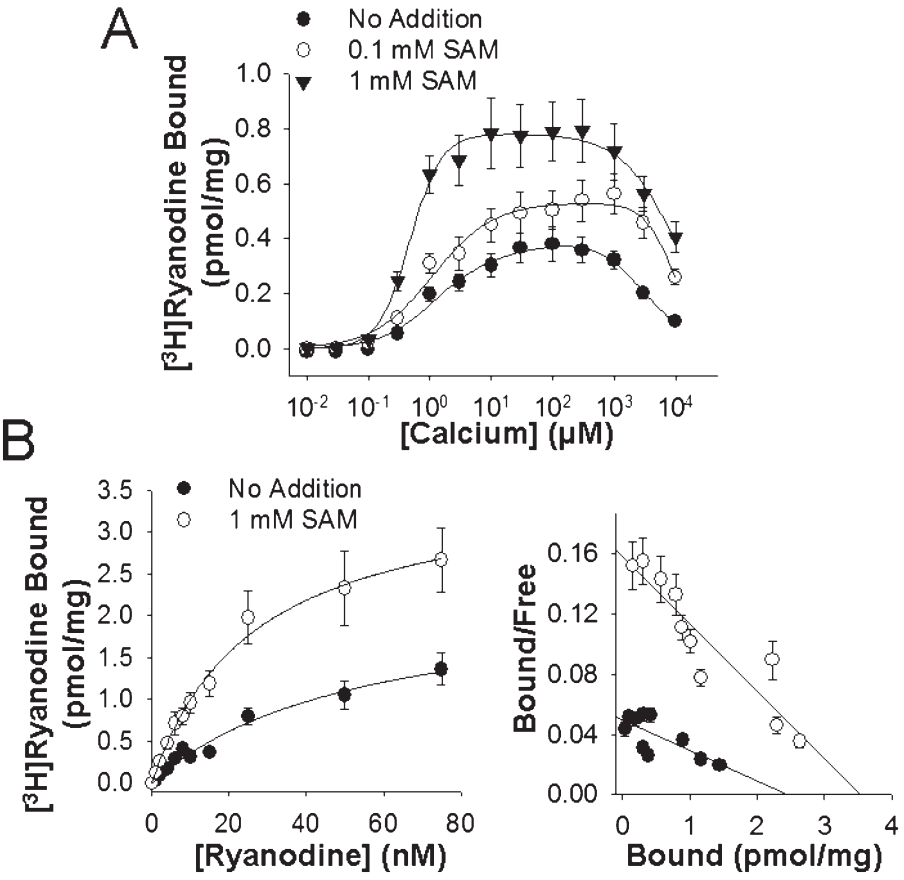

FIGURE 1: SAM enhances CSR vesicle [^{3}H]ryanodine binding. (A) The Ca^{2+} concentration dependence of CSR vesicle [^{3}H]ryanodine binding was performed as described in Materials and Methods in media containing the indicated Ca^{2+} concentration and either no addition, 0.1 mM SAM, or 1 mM SAM. [^{3}H]Ryanodine binding is expressed as picomoles of ryanodine bound per milligram of CSR protein. The solid lines are the fits to the Ca^{2+} concentration dependence; $n = 4$. (B) Saturation analysis of the effects of SAM on CSR [^{3}H]ryanodine binding was performed as described in Materials and Methods in the presence of 3 μM Ca^{2+} and the indicated concentration of ryanodine. Lines are fits to eq 2 (left panel). The right panel shows the Scatchard plot of the same data; $n = 7$. [^{3}H]Ryanodine binding is expressed as picomoles of ryanodine bound per milligram of CSR protein.

Table 1: Parameters from Fits to Ca^{2+} Concentration Dependence of CSR Vesicle [^{3}H]Ryanodine Binding[a]

	B' (pmol/mg)	EC_{50} (μM)	IC_{50} (mM)	n_a	n_i
no addition	0.38 ± 0.02	1.41 ± 0.34	3.8 ± 0.80	1.0 ± 0.20	1.19 ± 0.29
0.1 mM SAM	0.53 ± 0.02[c]	1.13 ± 0.25	9.61 ± 1.39[b]	0.89 ± 0.15	1.77 ± 0.62
1 mM SAM	0.78 ± 0.02[d]	0.47 ± 0.05[b]	10.1 ± 1.67[b]	1.71 ± 0.22	0.96 ± 0.19

[a]The Ca^{2+} concentration dependence of CSR vesicle [^{3}H]ryanodine binding was performed as described in Materials and Methods in media containing the indicated Ca^{2+} concentration and either no addition, 0.1 mM SAM, or 1 mM SAM. [b]$p \leq 0.05$. [c]$p \leq 0.005$. [d]$p \leq 0.001$ versus no addition.

[^{3}H]ryanodine binding revealed that SAM enhances Ca^{2+} activation of RyR2 (Figure 1A). The effects of 0.1 and 1 mM SAM on the maximal Ca^{2+}-induced CSR vesicle [^{3}H]ryanodine binding, EC_{50}, IC_{50}, n_a, and inhibition n_i are given in Table 1. In the presence of 0.1 mM SAM the B' and IC_{50} of CSR vesicle [^{3}H]ryanodine binding increased significantly. Inclusion of 1 mM SAM in the binding media increased the B' and IC_{50} and additionally decreased the EC_{50}. SAM did not significantly increase CSR [^{3}H]ryanodine binding in media containing subactivating Ca^{2+} concentrations ($\leq$0.1 μM). Thus, SAM did not alone activate RyR2 but enhanced Ca^{2+} activation of RyR2 and increased the Ca^{2+} concentration required to inhibit ryanodine binding. Saturation analysis was performed to determine the effects of SAM on the affinity of RyR2 for ryanodine and the number of channels which bind ryanodine (Figure 1B). In media containing 3 μM Ca^{2+}, B_{max} was increased from 2.45 ± 0.3 pmol/mg in the absence of SAM to 3.43 ± 0.3 pmol/mg in the presence of 1 mM SAM ($p = 0.047$, $n = 7$). SAM also significantly increased the CSR affinity for ryanodine, decreasing the K_d from 52.3 ± 13.2 nM in the absence of SAM to 21.4 ± 4.1 nM in the presence of 1 mM SAM ($p = 0.047$, $n = 7$).

Methyltransferase Inhibitors Do Not Block the SAM-Induced Increase in CSR Vesicle [^{3}H]Ryanodine Binding. SAM is the primary methyl group donor for the enzyme-mediated methylation of biological macromolecules. Activation of RyR2 by SAM may therefore be the result of protein methylation. *S*-Adenosyl-L-homocysteine (SAH), a product of methyl group transfer from SAM to an acceptor molecule, inhibits methyltransferase activity by mass action, while sinefungin inhibits transmethylation reactions by competing for the SAM binding site on methyltransferases. We investigated the effect of increasing concentrations of sinefungin and SAH on the SAM-induced increase in CSR vesicle [^{3}H]ryanodine binding. SAM increased CSR vesicle [^{3}H]ryanodine binding in media

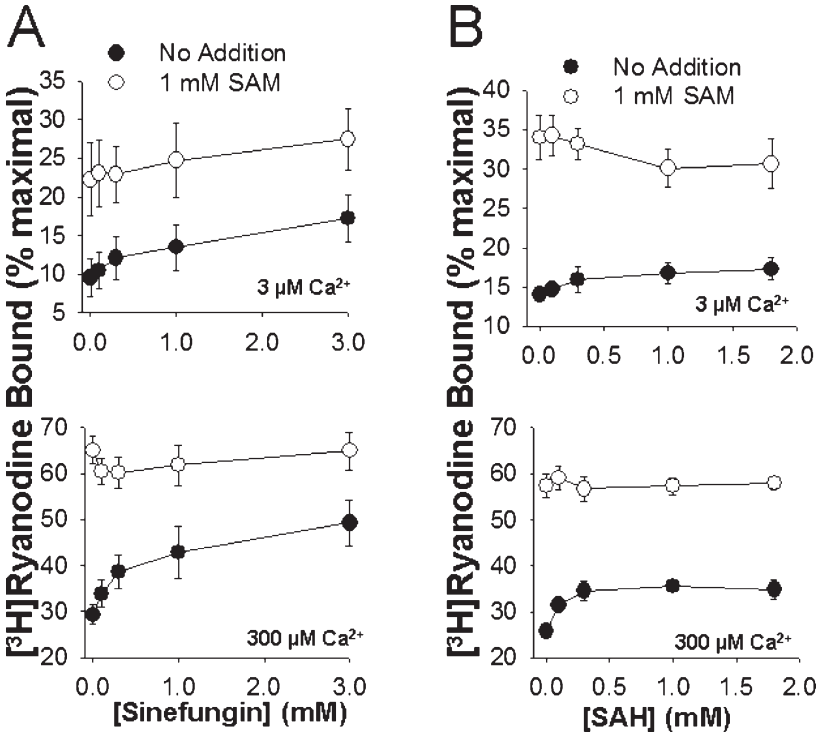

FIGURE 2: Methyltransferase inhibitors do not block SAM activation. (A) CSR vesicle [^{3}H]ryanodine binding was performed as described in Materials and Methods in media containing 3 μM Ca^{2+} (top panel; $B' = 2.9 \pm 0.2$ pmol/mg; $n = 4$) or 300 μM Ca^{2+} (bottom panel; $B' = 2.9 \pm 0.2$ pmol/mg; $n = 6$) and the indicated concentrations of sinefungin with or without (no addition) 1 mM SAM. In media containing 300 μM Ca^{2+}, 3 mM sinefungin alone increased [^{3}H]ryanodine binding ($p < 0.01$ vs sinefingin, no addition). (B) CSR vesicle [^{3}H]ryanodine binding was performed as described in Materials and Methods in media containing 3 μM Ca^{2+} (top panel; $B' = 2.5 \pm 0.3$ pmol/mg; $n = 4$) or 300 μM Ca^{2+} (bottom panel; $B' = 2.0 \pm 0.2$ pmol/mg; $n = 4$) and the indicated concentrations of SAH with or without (no addition) 1 mM SAM. In media containing 300 μM Ca^{2+}, SAH $\geq$ 0.1 mM alone increased [^{3}H]ryanoding binding ($p < 0.01$ vs SAH, no addition). [^{3}H]Ryanodine binding is expressed as percent of B' [^{3}H]ryanodine binding.

Table 2: Radioactivity Obtained (CPM, Counts Per Minute) from [^{3}H]SAM-Pretreated CSR and Immunoprecipitated RyR2[a]

incubation conditions	CSR (CPM)	RyR2 IP with antibody (CPM)	RyR2 IP without antibody (CPM)
[^{3}H]SAM alone	54676 ± 4823	196.7 ± 37.12	175.17 ± 17.14
+unlabeled SAM	1183 ± 92.26[b]	69.33 ± 25.39[c]	40.67 ± 11.08[d]
+SAH	2407 ± 299.5[b]	53.83 ± 13.57[c]	28.83 ± 3.77[d]
+unlabeled SAM + SAH	1750 ± 163.5[b]	46.17 ± 11.26[c]	33.67 ± 6.99[d]

[a]CSR was incubated as described in Materials and Methods. Data are means ± SE from three experiments (all assays were performed in duplicate). [b]$p \leq 0.001$. [c]$p \leq 0.01$. [d]$p \leq 0.05$ versus [^{3}H]SAM alone.

containing either 3 μM Ca^{2+} ($p = 0.055$) or 300 μM Ca^{2+} ($p < 0.001$), and the effect of SAM was not blocked by sinefungin up to 3 mM (Figure 2A). In Figure 2B SAM increased CSR vesicle [^{3}H]ryanodine binding in media containing either 3 or 300 μM Ca^{2+} ($p < 0.001$), and the addition of SAH up to 1.8 mM had no effect on the SAM-induced increase in binding. Due to low solubility of SAH, higher concentrations of the compound were not used. These results suggest activation of RyR2 by SAM is not the result of enzyme-mediated methylation. Alone, SAH and sinefungin caused a small increase in [^{3}H]-ryanodine binding in media containing 300 μM Ca^{2+}.

RyR2 Methylation Is Not Detected Following Incubation of CSR Vesicles with [^{3}H]SAM. Additional experiments were performed to determine if RyR2 is a target of SAM-mediated protein methylation. CSR vesicles were pretreated with *S*-adenosyl-L-[*methyl*-^{3}H]methionine ([^{3}H]SAM) in the presence or absence of SAH and/or excess unlabeled SAM, followed by centrifugation and washing to remove unincorporated [^{3}H]SAM. Radioactivity associated with pretreated CSR and retained in respective immunoprecipitates was determined as an indicator of [^{3}H]methyl group incorporation (Table 2, Figure 3). The inset in Figure 3 shows a representative Western blot as an indication of RyR2 protein yield obtained by our immunoprecipitation protocol. Inclusion of SAH and/or excess unlabeled SAM in the incubation buffer during [^{3}H]SAM treatment reduced CSR [^{3}H]methyl group incorporation (CPM, counts per minute) by ≥95%. The observation that [^{3}H]methyl group incorporation was inhibited by SAH indicates that methyltransferases are present in our CSR preparations and that SAH does indeed inhibit SAM-mediated methylation. Less than 6% of the radioactivity incorporated into pretreated CSR was retained by RyR2 immunoprecipitation. There was no difference in the amount of radioactivity recovered by immunoprecipitation performed in the presence or absence of a RyR2-specific antibody, indicating that [^{3}H]methyl groups retained by immunoprecipitation were not specific to RyR2. Therefore, RyR2 is not among the SR components methylated during SAM pretreatment.

Effects of SAM on CSR Vesicle [^{3}H]Ryanodine Binding in the Presence of Other Physiological RyR2 Effectors. To further characterize SAM activation of RyR2, we investigated

the effects of SAM on RyR2 regulation by Mg^{2+} and the nonhydrolyzable ATP analogue, AMPPNP, in media containing 3 μM, 300 μM, or 10 mM Ca^{2+} (Figure 4, Table 3). In the absence of other RyR2 regulators (Ca^{2+} alone) 1 mM SAM significantly increased CSR [^{3}H]ryanodine binding over control. In media containing 3 μM Ca^{2+}, the addition of 1 mM Mg^{2+} caused a reduction in CSR ryanodine binding in both the presence and absence of SAM. CSR vesicle [^{3}H]ryanodine binding was significantly enhanced by 1 mM AMPPNP at all three Ca^{2+} concentrations investigated; however, in media containing 1 mM SAM, the addition of AMPPNP did not cause a further increase in CSR [^{3}H]ryanodine binding. Thus, there is an interaction between SAM and AMPPNP activation of RyR2 as the combined effects of the two agonists are not additive.

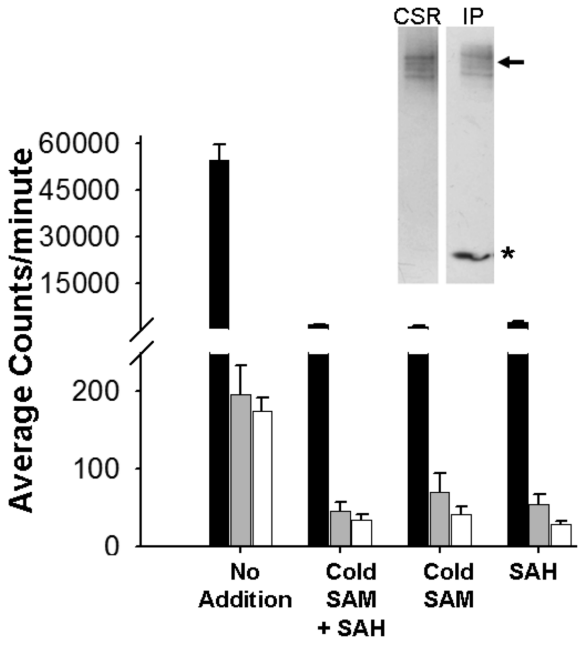

FIGURE 3: RyR2 is not methylated in the presence of SAM. CSR was incubated as described in Materials and Methods in the presence of 0.285 μM (3 μCi) [^{3}H]SAM and no addition or 1 mM SAH and/or 3.2 mM unlabeled SAM (>1000-fold excess). CSR vesicles were centrifuged through sucrose, washed, and resuspended 10% sucrose. RyR2 was immunoprecipitated from treated CRS either in the presence or in the absence of an RyR2 antibody. Liquid scintillation counting was used to measure radioactivity ([^{3}H]methyl groups) associated with 100 μg of treated CSR (black bars), and 20 μL aliquots of samples which were immunoprecipitated from treated CSR in the presence (gray bars) or absence (white bars) of anti-RyR2. The inset shows a Western blot demonstrating typical protein yield from RyR2 immunoprecipitations performed as described in Materials and Methods. The positions of RyR2 and RyR antibody are indicated with an arrow and asterisk, respectively. Data are means ± SE from three experiments (all assays were performed in duplicate).

SAM Competes with Adenine Nucleotide-Induced Increase in CSR Vesicle [^{3}H]Ryanodine Binding. Importantly, SAM contains an adenosine moiety and is therefore structurally similar to ATP and other adenine-based compounds (Figure 5). Thus, the interaction between SAM and AMPPNP activation of RyR2 provoked us to investigate more thoroughly whether SAM activation of RyR2 occurs via SAM interacting with the adenine nucleotide binding site(s). The substitution of AMPPNP for ATP avoids the potential confounding effect of RyR2 phosphorylation; however, differences in the efficacy of RyR activation by ATP and its nonhydrolyzable analogues have been noted (*3*, *23*). Thus, we compared the SAM, ATP, and AMPPNP concentration dependence of CSR vesicle [^{3}H]ryanodine binding (Figure 6A). The SAM and ATP concentration dependence of CSR [^{3}H]ryanodine binding paralleled one another up to 10 mM. Binding was significantly increased over control by all SAM concentrations ≥0.1 mM and by all ATP concentrations ≥0.3 mM. The extent of CSR [^{3}H]ryanodine binding was not different between SAM and ATP at any of the concentrations investigated. In contrast, AMPPNP was a much less potent RyR2 activator. The discrepancy between the ATP and AMPPNP concentration dependence of CSR [^{3}H]ryanodine binding motivated the use of ATP in subsequent experiments.

To determine whether SAM and ATP act via a common binding site, we investigated competition between the SAM- and adenine nucleotide-induced increase in CSR [^{3}H]ryanodine binding. Figure 6B shows the ADP concentration dependence of CSR [^{3}H]ryanodine binding performed in the absence (no addition) and presence of either 0.6 mM ATP or 0.6 mM SAM. In media containing 3 μM Ca^{2+}, ADP (≥1 mM) significantly increased CSR [^{3}H]ryanodine binding in a concentration-dependent manner, and ATP enhanced binding in the absence and presence of 1 mM ADP but had no further effect on binding at higher concentrations of ADP. The lack of an additive effect of ADP plus ATP is consistent with two ligands acting via a common site (the adenine nucleotide binding site(s)). Likewise, SAM enhanced

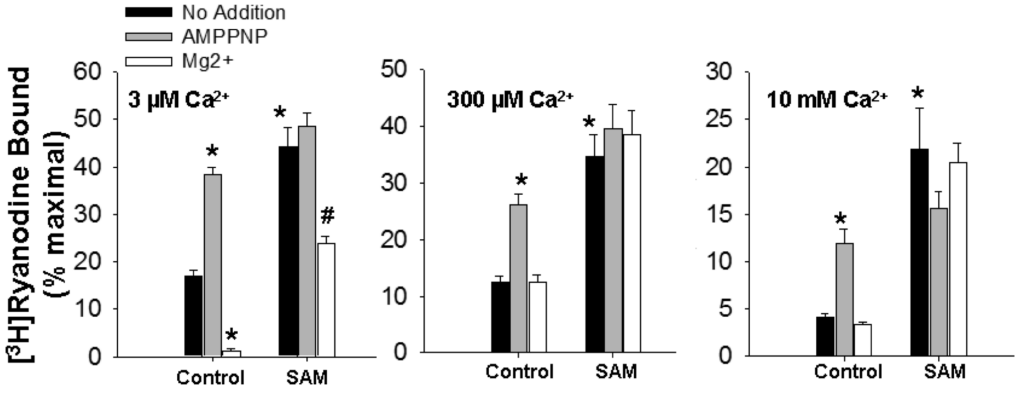

FIGURE 4: Effects of SAM on modulation of CSR vesicle [^{3}H]ryanodine binding by established RyR2 regulators. CSR vesicle [^{3}H]ryanodine binding was performed as described in Materials and Methods in media containing 3 μM Ca^{2+} (left panel; $B' = 1.5 \pm 0.4$ pmol/mg; $n = 5$), 300 μM Ca^{2+} (middle panel; $B' = 3.6 \pm 0.4$ pmol/mg; $n = 5$), or 10 mM Ca^{2+} (right panel; $B' = 3.6 \pm 0.4$ pmol/mg; $n = 5$) in the presence or absence (control) of 1 mM AMPPNP or 1 mM Mg^{2+} with or without (no addition) 1 mM SAM . *, $p \leq 0.001$ versus control, no addition; #, $p \leq 0.01$ versus SAM, no addition; [^{3}H]ryanodine binding is expressed as percent of B' [^{3}H]ryanodine binding.

Table 3: Effects of SAM on Modulation of Cardiac SR Vesicle [^{3}H]Ryanodine Binding by Established RyR2 Regulators[a]

	3 μM Ca^{2+}		300 μM Ca^{2+}		10 mM Ca^{2+}	
	control (% B')	SAM (% B')	control (% B')	SAM (% B')	control (% B')	SAM (% B')
no addition	17.0 ± 1.2	44.2 ± 4.1[b]	12.4 ± 1.1	34.6 ± 3.8[b]	4.1 ± 0.4	21.8 ± 4.4[b]
AMPPNP	38.3 ± 1.7[b]	48.6 ± 2.7	26.0 ± 2.1[b]	39.5 ± 4.4	12.0 ± 1.4[b]	15.6 ± 1.7
Mg^{2+}	1.09 ± 0.6[b]	23.8 ± 1.7[c]	12.5 ± 1.1	38.5 ± 4.3	3.3 ± 0.4	20.5 ± 2.0

[a]CSR vesicle [^{3}H]ryanodine binding was performed as described in Materials and Methods in media containing 3 μM Ca^{2+}, 300 μM Ca^{2+}, or 10 mM Ca^{2+} in the presence or absence (control) of 1 mM AMPPNP or 1 mM Mg^{2+} with or without (no addition) 1 mM SAM. [b]$p \leq 0.001$ versus control, no addition. [c]$p \leq 0.01$ versus SAM, no addition. [^{3}H]Ryanodine binding is expressed as percent of B' [^{3}H]ryanodine binding.

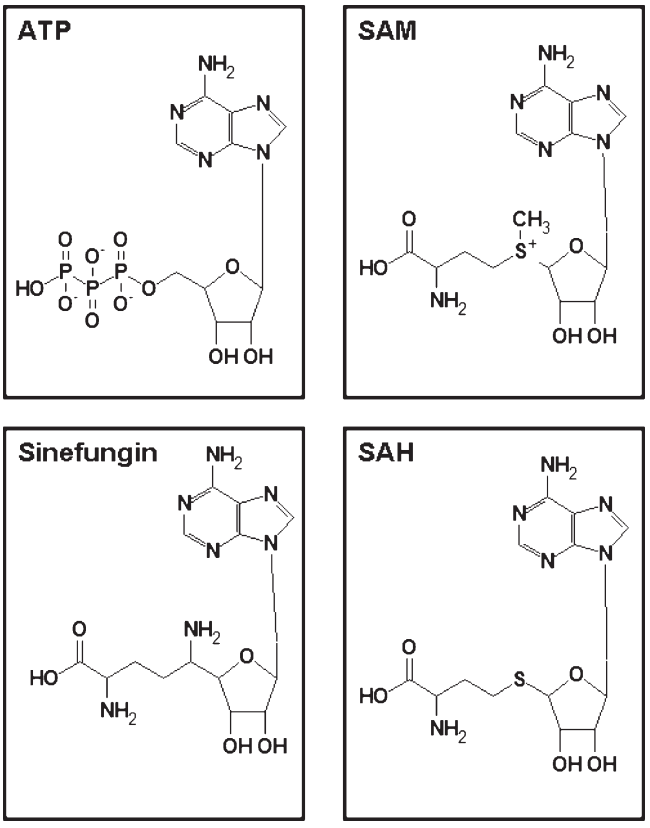

FIGURE 5: Chemical structures of ATP, *S*-adenosyl-L-methionine (SAM), *S*-adenosyl-L-homocysteine (SAH), and sinefungin. SAM is synthesized from methionine and ATP, which serves as an adenosine "donor". Note the sulfonium of SAM imparts a net positive charge to the molecule in contrast to the electronegative phosphates of ATP. The methyltransferase inhibitors SAH and sinefungin have no net charge and have minimal effect on CSR [^{3}H]ryanodine binding.

binding in the absence and presence of 1 mM ADP but had no additional effect in the presence of higher concentrations of ADP. We also found that a range of AMP concentrations did not potentiate either the ATP- or SAM-induced increase in CSR [^{3}H]ryanodine binding in media containing submaximally activating (10 μM), maximally activating (300 μM), or inhibitory (10 mM) Ca^{2+} concentration. AMP (≥5 mM) significantly increased CSR [^{3}H]ryanodine binding in a concentration-dependent manner, and ATP enhanced binding only in the absence of AMP. Comparably, SAM enhanced binding only in the absence of AMP in media containing 300 μM and 10 mM Ca^{2+}. In media containing 10 μM Ca^{2+}, SAM enhanced ryanodine binding in the absence and presence of 5 mM AMP but had no further effect on binding at higher concentrations of AMP (Figure 6C). Taken together, the data presented in Figure 6 suggest that SAM and adenine nucleotides act through a common binding site.

SAM Activates RyR2 and Increases Subconductance Level Openings. As a more direct measure of SAM-induced channel opening, we examined the effects of SAM on native RyR2 channels incorporated into phospholipid bilayers. Consistent with results from CSR [^{3}H]ryanodine binding, 0.1 mM SAM activated RyR2, which was reflected by a significant increase in channel open probability (P_o). In the experiment shown in Figure 7, channel P_o increased from 0.087 in the presence of 10 μM *cis* Ca^{2+} to 0.271 after the addition of 0.1 mM *cis* SAM. The increase in P_o could be attributed to both an increase in the mean open time (control = 0.45 ms; 0.1 mM SAM = 1.00 ms) and a decrease in the mean closed time (control = 6.35 ms; 0.1 mM SAM = 2.66 ms). The summary data presented in Table 4 and Figure 10 support the conclusion that 0.1 mM SAM caused a significant increase in mean open time. Additionally, mean channel closed time was decreased in the presence of 0.1 mM SAM in three out of four experiments.

To further investigate whether SAM interacts with the RyR2 adenine nucleotide binding site, we compared the effects of SAM and ATP on the activity of native RyR2 channels. An identical concentration of SAM and ATP shown to substantially activate RyR2 (2 mM) was chosen for comparison, given the overlap in the SAM and ATP concentration dependence of CSR vesicle [^{3}H]ryanodine binding (Figure 6A). Activation of RyR2 was reflected by a significant increase in channel P_o after the addition of either ATP or SAM to the *cis* chamber. Representative RyR2 channel current recordings are shown in Figure 8. Channel P_o increased from 0.0049 in the presence of 10 μM *cis* Ca^{2+} to 0.022 after the addition of 2 mM *cis* ATP (Figure 8A). The increase in P_o was due to an increase in the mean open time (control = 0.94 ms; 2 mM ATP = 1.57 ms) and a decrease in the mean closed time (control = 205 ms; 2 mM ATP = 96.8 ms). Variability is a common occurrence in single channel behavior. Wide variability in ligand-activated channel P_o values has previously been observed for both cardiac and skeletal RyRs (*24*, *25*) and Ca^{2+}-activated K^+ channels (*26*). Although the channel shown in Figure 8B was activated to a greater extent by Ca^{2+} alone (P_o = 0.193) compared to the previous channel in 8A, the addition of 2 mM *cis* SAM caused an increase in P_o to 0.290. Notably, SAM activation of RyR2 was not time dependent. During RyR2 current recording experiments, increases in channel P_o were observed immediately following the addition of either ATP or SAM to the *cis* chamber with ~10 s stirring. Plots of channel P_o throughout the course of representative experiments show that P_o increased immediately upon the addition of either SAM or ATP to the cis chamber (Figure 8C−E). Although fluctuations in channel P_o occur through out the experiment, no consistent trend for channel P_o to either increase or decrease upon extended (~2 min) exposure to SAM or ATP was observed.

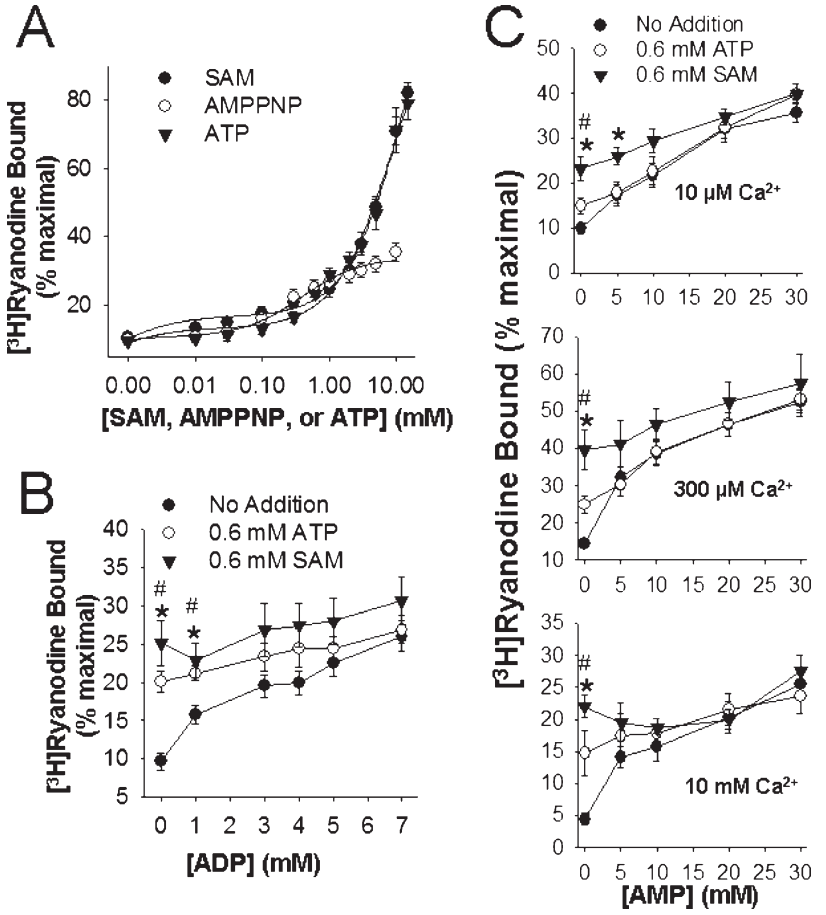

FIGURE 6: Interaction between SAM and ATP activation of RyR2. (A) Comparison of the SAM, AMPPNP, and ATP concentration dependence of CSR [^{3}H]ryanodine binding performed in the presence of 3 μM Ca^{2+} ($B' = 2.4 \pm 0.3$ pmol/mg; $n = 5$). (B) Competition between ADP and SAM or ATP-induced increase in CSR [^{3}H]ryanodine binding was performed in media containing 3 μM Ca^{2+} and the indicated concentrations of ADP with or without (no addition) 0.6 mM ATP or 0.6 mM SAM ($B' = 2.7 \pm 0.15$ pmol/mg; $n = 5$). *, $p \leq 0.05$ for 0.6 mM SAM versus no addition; #, $p \leq 0.05$ for 0.6 mM ATP versus no addition. (C) Competition between AMP and SAM or ATP-induced increase in CSR [^{3}H]ryanodine binding was performed in media containing 10 μM Ca^{2+} (top panel; $B' = 3.8 \pm 0.7$ pmol/mg; $n = 5$), 300 μM Ca^{2+} (middle panel; $B' = 3.3 \pm 0.6$ pmol/mg; $n = 4$), or 10 mM Ca^{2+} (bottom panel; $B' = 3.3 \pm 0.6$ pmol/mg; $n = 4$) and the indicated concentrations of AMP with or without (no addition) 0.6 mM ATP or 0.6 mM SAM. *, $p \leq 0.05$ for 0.6 mM SAM versus no addition; #, $p \leq 0.05$ for 0.6 mM ATP versus no addition. [^{3}H]Ryanodine binding is expressed as percent of B' [^{3}H]ryanodine binding.

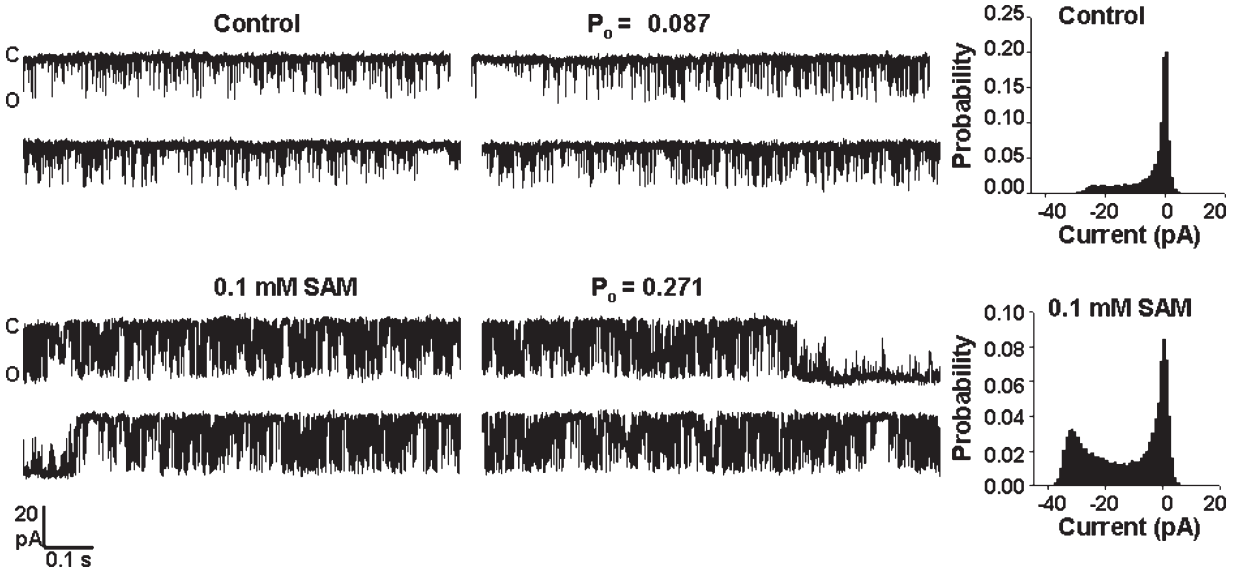

FIGURE 7: SAM activates native RyR2 channels. Currents were recorded in symmetrical 250 mM Cs^+ using a pulsing protocol consisting of steps to −70 mV. Closed (C) and full conductance open (O) levels are indicated to the left of the traces, and corresponding amplitude histograms from ≥2 min recording time are shown to the right. Channel open probability (P_o) is indicated above each trace. The top trace shows a representative channel activated by 10 μM *cis* Ca^{2+}, and the bottom trace shows activity of the same channel immediately following the addition of 0.1 mM *cis* SAM.

Table 4: Effects of ATP and SAM on Mean Channel Open and Closed Times[a]

	mean open time before addition (ms)	mean open time after addition (ms)	mean closed time before addition (ms)	mean closed time after addition (ms)
2 mM ATP	0.73 ± 0.16	1.32 ± 0.33	87.77 ± 58.65	36.13 ± 30.39
2 mM SAM	0.86 ± 0.10	2.47 ± 0.82	28.17 ± 19.11	6.13 ± 3.33
0.1 mM SAM	0.57 ± 0.11	1.12 ± 0.20[b]	6.73 ± 2.44	2.89 ± 1.23

[a]Single RyR2 channel currents were recorded in the presence of 10 μM *cis* Ca^{2+} and analyzed for mean open and closed times as described in Materials and Methods before and after the addition of 2 mM ATP, 2 mM SAM, or 0.1 mM SAM to the *cis* chamber. Data in each cell are means ± SE from four experiments. [b]$p \leq 0.05$ versus mean open time before addition.

In agreement with previously described effects of ATP on RyR2 (*27*), single channel data indicate that 2 mM *cis* ATP enhanced channel P_o through both an increase in mean open time and a decrease in mean closed time. In the representative single channel experiment shown in Figure 8A, mean channel open time increased from 0.94 to 1.57 ms and mean closed time decreased from 205 to 96.8 ms after the addition of 2 mM *cis* ATP. For the channel shown in Figure 7, 0.1 mM SAM increased the mean open time from 0.45 to 1.00 ms and decreased the mean closed time from 6.35 to 2.66 ms. After the addition of 2 mM *cis* SAM (Figure 8B) mean channel open time increased from 0.919 to 3.13 ms and mean closed time decreased from 4.1 to 1.45 ms. Thus, the effects of 0.1 and 2 mM SAM on RyR2 mean open and closed times followed similar trends to those observed for ATP (Table 4, Figure 10C−E).

In contrast to ATP, however, SAM activation of RyR2 was associated with a marked change in channel conductance, as evidenced in the current trace and corresponding amplitude histogram shown in Figure 8B (bottom trace). Average maximal single RyR2 channel unitary conductance (γ_{max}) in 250 mM symmetrical Cs^+ recorded at −70 mV was 513 ± 10, 514 ± 15, 507 ± 16, and 528 ± 28 pS for control, 0.1 mM SAM, 2 mM SAM, and 2 mM ATP, respectively. The average conductance of substate openings in the presence of 2 mM SAM was 294 ± 22 pS corresponding to ~60% of γ_{max}. Figure 9A shows that the SAM-induced subconductance state persists following the addition of ATP. RyR2 channel transitions between the closed, maximum conductance, and the SAM-induced subconductance state are more clearly resolved in segments of channel recording shown on an expanded time scale (Figure 9B). In the presence of 2 mM *cis* SAM, entry into the subconductance state occurred either from the closed or from the fully open state (arrows in Figure 9B). Both of these transitions were commonly observed. The summary data in Figure 10B show that in the presence of 2 mM SAM the percent of channel openings to a predominant substate of ~60% γ_{max} increased from 1.7 ± 1.2% to 31.3 ± 5%, while ATP had no effect on the percent of substate openings (control, 1.2 ± 0.5%; 2 mM ATP, 0.4 ± 0.2%). Substates detected under control conditions likely reflect very brief openings that were not fully resolved. The percent of RyR2 substate openings also increased in the presence of 0.1 mM SAM (control = 0.14 ± 0.08%; 0.1 mM SAM = 1.54 ± 0.15% substate openings) (Figure 10B); however, due to the low frequency of occurrence, these events are difficult to resolve visually (Figure 7).

Potential Mechanisms of the SAM-Induced Subconductance State. Attempts were made to remove SAM by perfusion of the *cis* chamber; however, this procedure produced inconsistent results including substantial increases and declines in channel P_o. Thus, as an alternative approach to test the reversibility of the SAM-induced RyR2 substate, we performed a subset of experiments in which native RyR2 from heavy CSR treated with or without SAM were incorporated into phospholipid bilayers. Representative current recordings from these experiments are shown in Figure 11. Prior incubation with 2 mM SAM altered RyR2 conductance with five out of seven channel recordings exhibiting a predominant substate of ~60% γ_{max} (Figure 11B). This predominant substate was not observed in any channel recordings (five recordings) from CSR incubated in the absence of SAM (Figure 11A), thus suggesting SAM alters RyR2 conductance via an indirect mechanism distinct from binding RyR2 adenine nucleotide site(s). In a previous study, Chen and colleagues proposed that SAM activation of RyRs from smooth muscle occurs via dissociation of FKBP (*10*). We therefore investigated whether SAM induced the dissociation of FKBP12.6 from RyR2. After pretreatment of CSR vesicles with SAM (0, 0.1, or 2 mM) at 37 °C for 30 min, the amount of FKBP12.6 associated with CSR vesicles was visualized by Western blots of CSR proteins immunostained with RyR2 or FKBP12.6 specific antibodies (Figure 12B). Immunostaining of the FKBP12.6 band (~12 kDa) was not reduced by incubation of CSR with 0.1 or 2 mM SAM. We also investigated whether the association between FKBP12.6 and RyR2 was required for the ATP- and SAM-induced increase in CSR vesicle [^{3}H]ryanodine binding. For this purpose, CSR vesicles were incubated in the absence (control treated) or presence (FK506 treated) of FK506, an immunosuppressant which has been shown to remove FKBPs from RyRs (*28*). FK506 treatment did not affect the SAM (Figure 12A, top panel) or ATP (Figure 12 A, bottom panel) concentration-dependent increase in CSR [^{3}H]ryanodine binding, further supporting the conclusion that FKBP12.6 dissociation is not the mechanism underlying SAM regulation of RyR2. Given the irreversible nature of the SAM-induced RyR2 subconductance state (Figure 11) we envision that SAM reduces RyR2 conductance via a mechanism distinct from binding the adenine nucleotide site(s).

DISCUSSION

We have used [^{3}H]ryanodine binding to SR vesicles recovered from cardiac tissue and RyR2 channel current recordings to study SAM regulation of RyR2. SAM activates RyR2 in a concentration-dependent manner. While physiological concentrations of SAM (0.1 mM) enhanced CSR vesicle [^{3}H]ryanodine binding by increasing the affinity of RyR2 for ryanodine (*14*), 1 mM SAM enhanced binding by increasing both the affinity of RyR2 for ryanodine and the number of channels which bind ryanodine (Figure 1B). Neither 0.1 or 1 mM SAM increased CSR [^{3}H]ryanodine binding in the presence of ≤0.1 μM Ca^{2+} but rather enhanced RyR2 Ca^{2+} activation (Figure 1B, Table 1). Thus SAM activation required the presence of activating concentrations of Ca^{2+}.

SAM participates in the methylation of proteins and other macromolecules, a mechanism by which the localization and

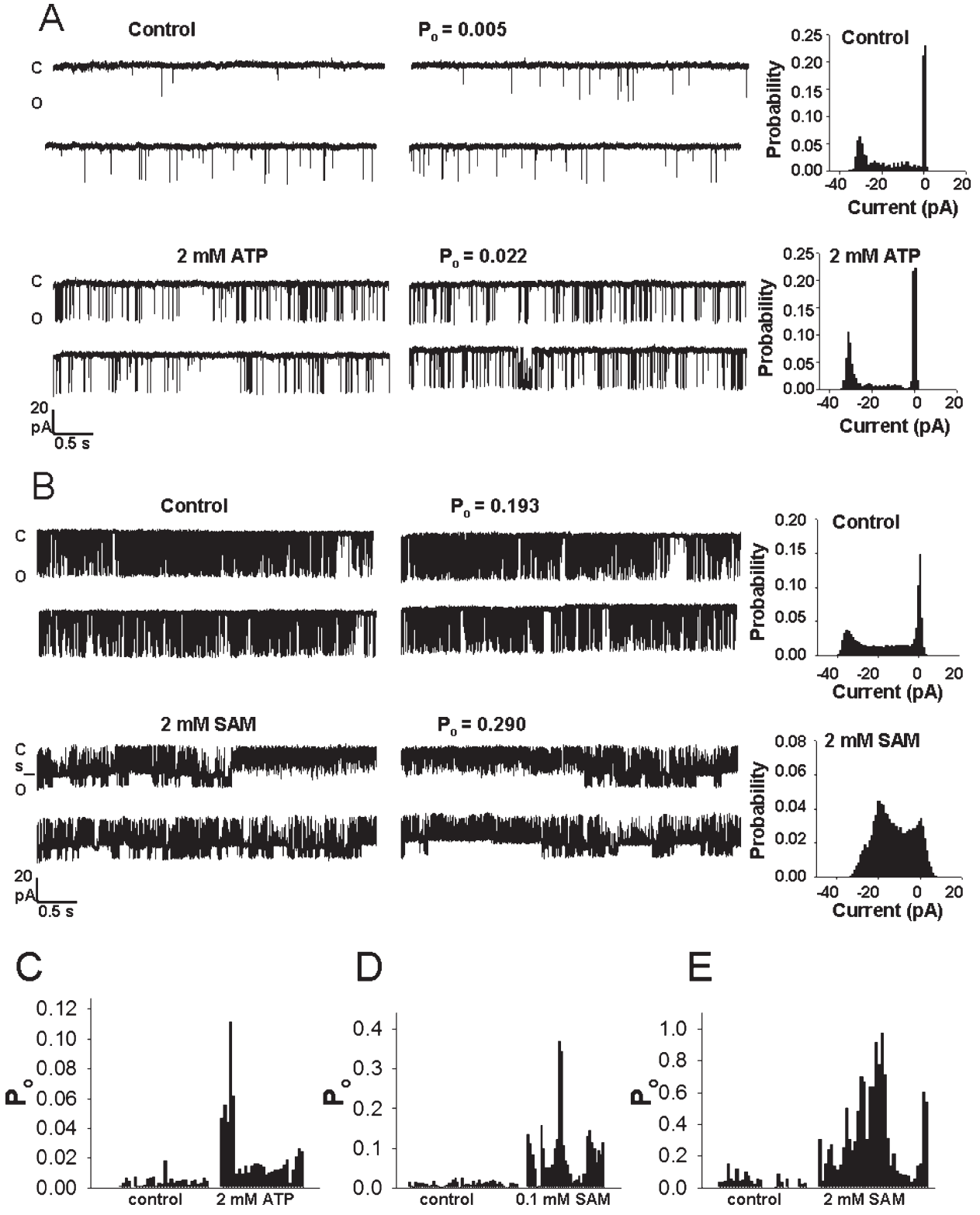

FIGURE 8: Comparison of SAM and ATP activation of native RyR2 channels. Currents were recorded in symmetrical 250 mM Cs^+ using a pulsing protocol consisting of steps to −70 mV. Closed (C), full conductance open (O), and subconductance open (s) levels are indicated to the left of the traces, and corresponding amplitude histograms from ≥2 min recording time are shown to the right. Channel open probability (P_o) is indicated above each trace. Top traces in each panel show a representative channel activated by 10 μM *cis* Ca^{2+}, and bottom traces show channel activity immediately following the addition of (A) 2 mM *cis* ATP or (B) 2 mM *cis* SAM. The SAM-induced subconductance state in (B) is typical and was observed in all experiments (six single channel recordings) upon addition of 2 mM SAM but was extremely rare upon the addition of 2 mM ATP. (C−E) Diary plots of P_o during successive 4 s sweeps. Data are from single experiments during which currents were recorded at −70 mV in symmetrical 250 mM Cs^+ before and after the addition of (C) 2 mM *cis* ATP, (D) 0.1 mM *cis* SAM, or (E) 2 mM *cis* SAM.

function of biological targets are altered (*2*). A diverse class of enzymes known as methyltransferases catalyzes the transfer of the methyl group from the sulfonium of SAM to the oxygen, nitrogen, or sulfur atom of biological targets (*3*). We therefore investigated whether SAM activation of RyR2 is associated with channel methylation by incubation of CSR vesicles with SAM

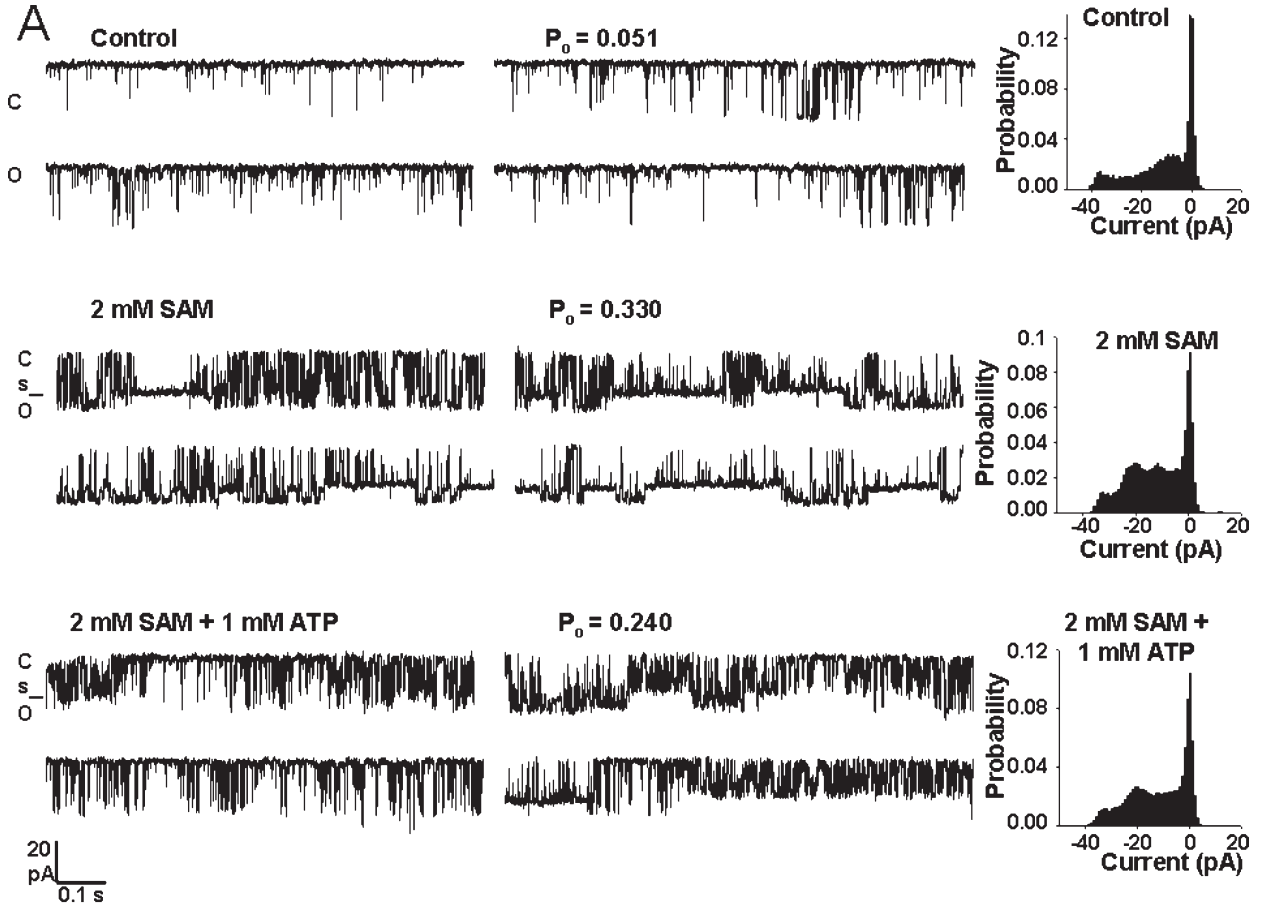

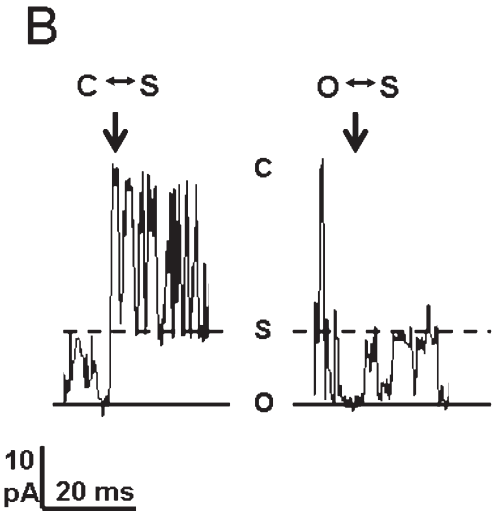

FIGURE 9: The SAM-induced subconductance state persists in the presence of ATP. (A) Currents were recorded in symmetrical 250 mM Cs^+ using a pulsing protocol consisting of steps to −70 mV. Closed (C), full conductance open (O), and subconductance open (s) levels are indicated to the left of the traces, and corresponding amplitude histograms from ≥2 min recording time are shown to the right. Channel open probability (P_o) is indicated above each trace. Traces are from a single channel activated by 10 μM Ca^{2+} (top), following the addition of 2 mM *cis* SAM (middle) and following the subsequent addition of 1 mM *cis* ATP (bottom). (B) Segments of channel recording following the addition of 2 mM *cis* SAM are shown on an expanded time scale. Transitions from the closed state (C) to the subconductance state (S and dotted line) and from the full conductance (O and solid line) to the subconductance state were frequently observed (arrows). The sequence of transitions between states is indicated above each arrow.

containing a radiolabeled methyl group. Inclusion of the methyltransferase inhibitor SAH and/or excess unlabeled SAM in the incubation buffer reduced the amount of radioactivity ([^{3}H]-methyl groups) incorporated into CSR vesicles by ≥95%, indicating (i) methyltransferases are present in our CSR preparations and (ii) SAM provides methyl groups for methylation of CSR components. However, immunoprecipitation of RyR2 from solubilized [^{3}H]SAM-treated CSR showed that the amount of radioactivity associated with RyR2 was negligible and nonspecific given that no difference was found compared to samples from immunoprecipitations performed in the absence of an RyR2-specific antibody (Table 2, Figure 3). Furthermore, inclusion of the

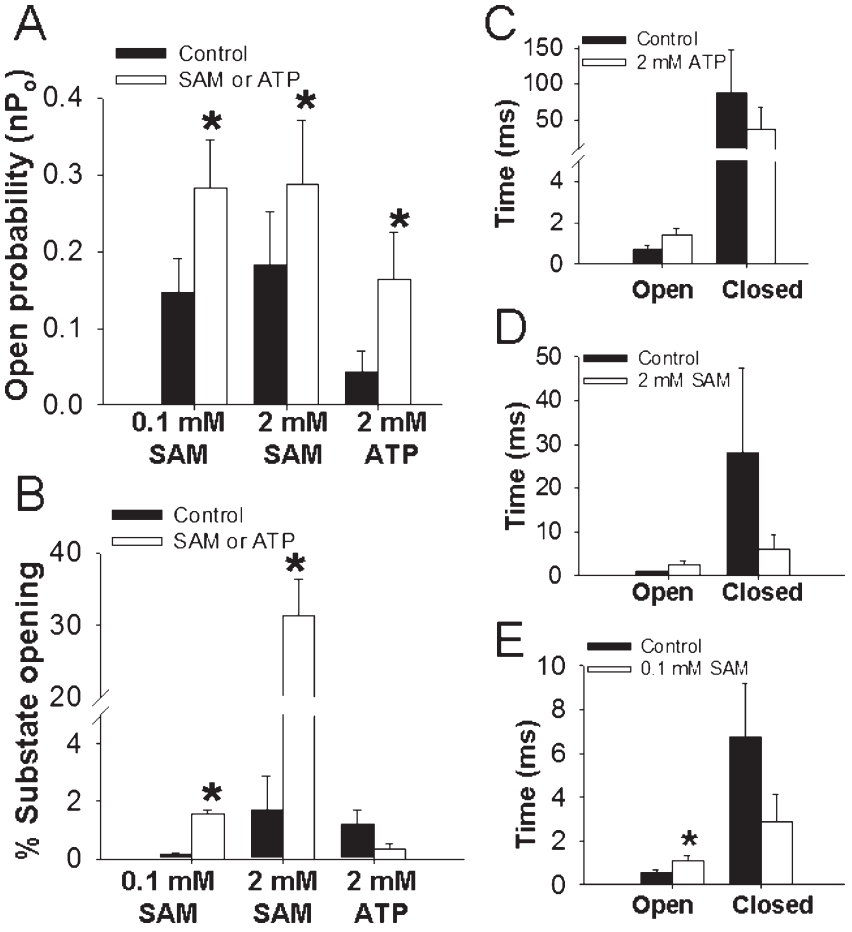

FIGURE 10: Effects of SAM and ATP on RyR2 activation and conductance. RyR2 channel currents were recorded in the presence of 10 μM *cis* Ca^{2+} (control) and following the addition of the indicated concentrations of *cis* ATP or SAM and analyzed as described in Materials and Methods for the following parameters: (A) channel P_o ($n = 6-12$), (B) single RyR2 % substate opening ($n = 4-5$), and (C−E) single RyR2 mean open and closed times ($n = 4$). *, $p \leq 0.05$ versus control.

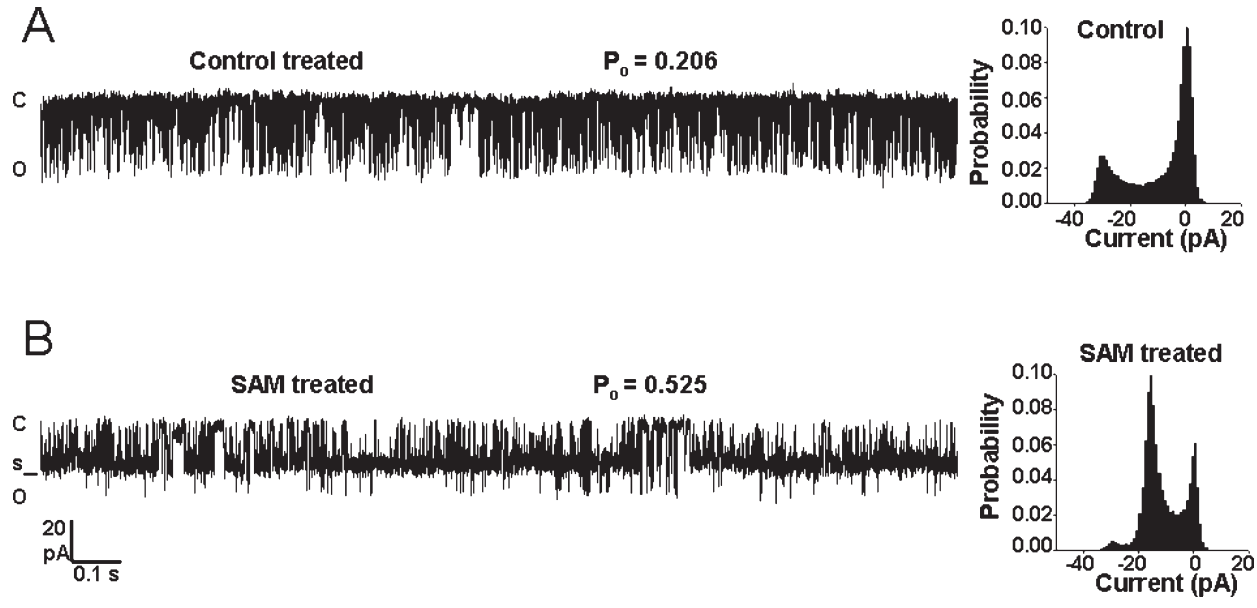

FIGURE 11: RyR2 from SAM-treated CSR exhibit altered conductance. Native RyR2 from heavy CSR incubated as described in Materials and Methods in the (A) absence or (B) presence of 2 mM SAM were incorporated into phospholipid bilayers. CSR was washed to remove SAM prior to RyR2 incorporation. Currents were recorded in symmetrical 250 mM Cs^+ using a pulsing protocol consisting of steps to −70 mV. Closed (C), full conductance open (O), and subconductance open (s) levels are indicated to the left of the traces, and corresponding amplitude histograms from ≥2 min recording time are shown to the right. Channel open probability (P_o) is indicated above each trace.

methyltransferase inhibitors SAH or sinefungin in the binding media did not prevent the SAM-induced increase in CSR [^{3}H]ryanodine binding (Figure 2). Together, these data suggest SAM activation of RyR2 does not involve channel methylation.

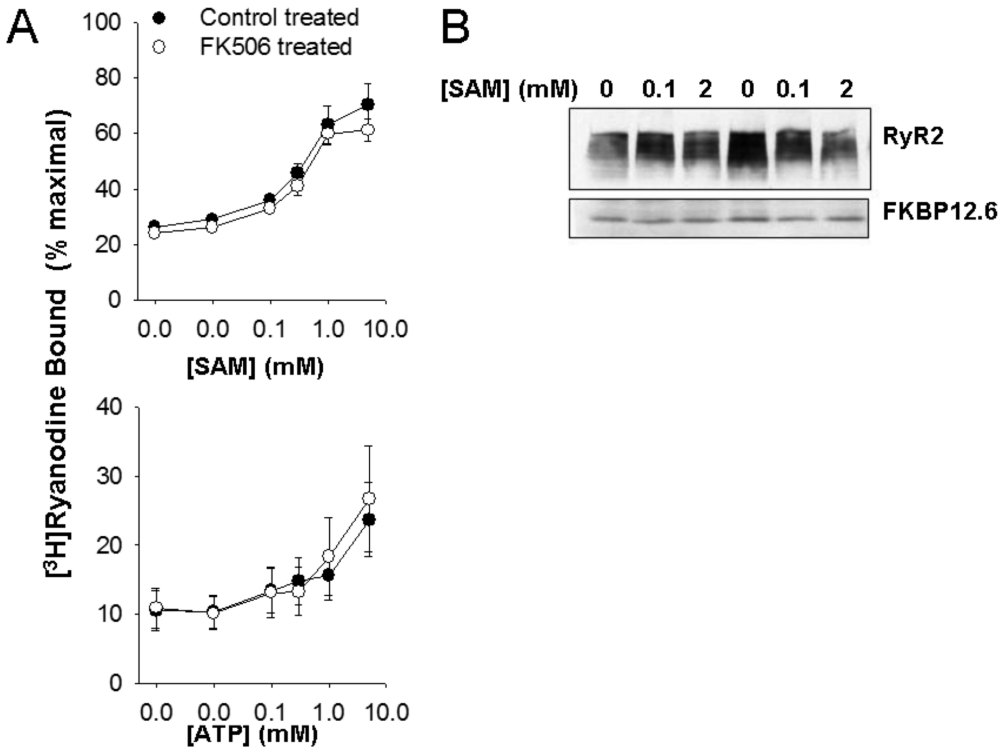

FIGURE 12: FKBP12.6 dissociation does not underlie the SAM-related RyR2 subconductance state. (A) Ryanodine binding to pretreated CSR was performed as described under Materials and Methods in media containing 10 μM Ca^{2+} and the indicated concentration of SAM (top panel; $B' = 2.3 \pm 0.4$; $n = 4$) or ATP (bottom panel; $B' = 5.4 \pm 0.9$; $n = 4$). [^{3}H]Ryanodine binding is expressed as a percent of maximal [^{3}H]ryanodine binding. FKBP506 treatment did not alter the SAM or ATP dependence of CSR [^{3}H]ryanodine binding. (B) CSR vesicles were incubated as described in Materials and Methods in the presence of 0, 0.1, or 2 mM SAM. Treated CSR vesicles were centrifuged through 15% sucrose, washed, and resuspended in a minimal volume of 10% sucrose. CSR was subjected to SDS−PAGE followed by Western blot analysis using antibodies specific for RyR2 and FKBP12.6. Western blot analysis indicates that SAM did not induce the loss of FKBP12.6 from CSR.

A point of interest is the structural similarity between SAM and ATP (Figure 5), an important physiological regulator of RyR2. Like ATP and its nonhydrolyzable analogue AMPPNP, SAM contains an adenosine moiety raising the possibility that SAM regulates RyR2 via the adenine nucleotide binding site(s). Analogous to adenine nucleotide regulation of RyR2 (*3*), SAM alone has little effect on channel activity in the absence of Ca^{2+} but enhances Ca^{2+} activation of the channel (Figure 1A). Furthermore, both SAM and AMPPCP similarly affect RyR2 ryanodine affinity and the number of channels that bind the ligand (Figure 1B) (*29*). Using CSR [^{3}H]ryanodine binding, we found that SAM did not potentiate activation of RyR2 by the nonhydrolyzable ATP analogue, AMPPNP, suggesting that SAM acts as an agonist at the ATP sites (Figure 4). Competition experiments were designed to further investigate the interaction between SAM and adenine nucleotide activation of RyR2. ATP did not potentiate the ADP- or AMP-induced increase in CSR [^{3}H]ryanodine binding, a finding consistent with agonists acting though a common binding site. Likewise, SAM did not potentiate RyR2 activation by ADP or AMP (Figure 6), suggesting that SAM acts through binding either the RyR2 adenine nucleotide binding site or a distinct but interacting site on the channel.

Single channel current recordings and analysis are routinely used to clarify the mechanisms underlying channel regulation. A principal goal of the present study, therefore, was to compare the effects of SAM and ATP on RyR2 channel gating using native RyR2 incorporated into phospholipid bilayers. In addition to 0.1 mM SAM, we chose a higher concentration of SAM and ATP (2 mM) shown though [^{3}H]ryanodine binding to produce substantial activation of RyR2 (Figure 6A). Single channel analyses showed that the effects of SAM on RyR2 P_o, mean open, and closed times followed similar trends to those observed for ATP (Table 4, Figure 10C−E). However, unlike ATP, SAM affected RyR2 channel conductance. A concentration-dependent increase in the proportion of channel openings to a subconductance level of ~60% γ_{max} was observed in the presence of 0.1 and 2 mM SAM (Figure 10B), with a much more pronounced effect observed with 2 mM SAM. A time-dependent effect of SAM would be expected if the mechanism involved an enzymatic process, e.g., protein methylation. However, the effects of SAM and ATP on native RyR2 channels were immediate and not time dependent, and the effects of SAM on RyR2 regulation appear independent of methylation as inhibitors of methyltransferase activity did not block the SAM-induced increase in CSR [^{3}H]ryanodine binding (Figure 2).

Interestingly, we observed that prior incubation of CSR with SAM caused lasting effects on RyR2 conductance while identical treatment of CSR in the absence of SAM was without effect (Figure 11). In these experiments, a wash step was included to remove SAM prior to channel incorporation; thus, a mechanism distinct from ligand binding likely underlies the SAM-induced RyR2 subconductance state. In its native membrane the RyR2 is part of a macromolecular complex in association with a number of accessory proteins implicated in channel modulation and signaling molecules involved in posttranslational protein modification (*30*). It is plausible that SAM alters the interaction between RyR2 and one or more endogenous effector proteins thereby affecting channel conductance. The RyR accessory protein FKBP12/12.6 is associated with RyRs in a 4:1 ratio with one FKBP bound to each RyR monomer. Removal of FKBP12

from the skeletal isoform of the channel (RyR1) increases channel activity and is associated with an increased frequency of subconductance openings (*17*, *31*). However, whether removal of FKBPs from RyR2 results in a similar alteration of channel behavior is unclear (*32*, *33*). Chen and colleagues attributed SAM activation of smooth muscle RyRs to FKBP methylation causing its dissociation from the channel (*10*). In an attempt to determine whether FKBP dissociation is involved in the SAM-related RyR2 subconductance state, we performed Western blot analysis of CSR proteins and found that immunostaining of the FKBP12.6 band was not reduced by incubation of CSR with 0.1 or 2 mM SAM (Figure 12B). In addition, there was no difference in the SAM-induced increase in [^{3}H]ryanodine binding to FK506-treated and control-treated CSR (Figure 12A). We were also unable to detect RyR2 methylation (Figure 3) or an effect of methyltransferase inhibitors on SAM activation of RyR2 (Figure 2). As opposed to smooth muscle in which all three RyR isoforms are expressed, RyR expression in cardiac muscle is nearly exclusively RyR2 (*11*−*13*). Therefore, the different populations of RyR channel isoforms studied, as well as tissue specific expression of methyltransferases, may account for the discrepancies between our data and reports by Chen et al.

The ability of ATP and its metabolites to activate RyR2 (efficacy) decreases in the order ATP > ADP > AMP > adenine > adenosine (*27*, *34*). Although the purine ring is important for agonist activity (*3*), the structural features of adenosine-based compounds which impart efficacy in activating RyR2 are unknown. Several lines of evidence suggest SAM activates RyR2 via the adenine nucleotide binding site(s): (i) SAM contains an adenosine group, (ii) RyR2 activation by SAM and adenine nucleotides is similar in that both compounds enhance Ca^{2+} activation of the channel but have minimal effects on channel activity in the absence of Ca^{2+} (*3*), (iii) millimolar concentrations of SAM and AMPPCP increase B_{max} and decrease the K_d for ryanodine, (iv) the SAM and ATP concentration dependence of CSR ryanodine binding overlap, (v) SAM does not potentiate adenine nucleotide activation of RyR2, and (vi) SAM and ATP have similar effects on mean channel open and closed times.

Studies using native RyR2 channels in phospholipid bilayers have demonstrated that decreasing the number of phosphate groups decreased the ability of adenosine-based compounds to activate the channel (*27*, *34*). Additional research has used comparative molecular field analysis to correlate the chemical structure of adenosine-based molecules with their ability to activate RyR2. This work showed that changes in electrostatic field and steric factors account for 64% and 36%, respectively, of the total correlation between structure and function. Increasing positive electrostatic potential of the molecule in diffuse regions corresponding to the phosphate groups of ATP was strongly correlated with increasing P_o; meanwhile, increasing negative electrostatic potential distal to the γ-phosphate was correlated with increasing P_o. Thus, the effect of electrostatic field on the conformational state of RyR2 is apparently complex. Nevertheless, the high efficacy of ATP was primarily attributed to the negative electrostatic field established by its ionized phosphate groups (*35*). SAM contains a positively charged sulfonium located in the region of the molecule corresponding to the α-phosphate in ATP (Figure 6) yet is equally effective as ATP in activating RyR2. Therefore, our proposal that SAM activates RyR2 via the adenine nucleotide binding site challenges the interpretation that high ligand efficacy at the adenine nucleotide site(s) requires a negative electrostatic potential. The methyltransferase inhibitors used in this study (sinefungin and SAH) are adenosine-based compounds which have no net charge (Figure 6). Sinefungin and SAH had minimal effects on RyR2 activity (Figure 2), an observation which is in accord with an important role of electrostatic interactions in the process of nucleotide activation of RyR2. Our data shed new light on the structure−activity relationship underlying adenine nucleotide regulation of RyR2 and suggest a potential use of SAM as a tool to clarify the structural basis for ligand affinity and efficacy at the adenine nucleotide site(s).

Interventions to increase intracellular SAM concentrations were shown to have a positive ionotropic effect in the heart which was at least partially attributed to activation of the SR Ca^{2+} pump (SERCA) upon SAM-dependent N-methylation of membrane phospholipids (*8*, *36*). Indeed, investigations of the effect phospholipid N-methylation has on RyR2 activity are few; however, the observed inability of methyltransferase inhibitors to block the SAM-induced increase in CSR [^{3}H]ryanodine binding suggests methyltransferase activity, and thus methylation, is not involved in SAM activation of RyR2. The virtual overlap in the SAM and ATP concentration dependence of CSR [^{3}H]ryanodine binding indicates that both the affinity of SAM for RyR2 and its ability to open the channel are comparable to that of ATP. Therefore, if SAM acts through binding the adenine nucleotide site(s) on RyR2, SAM would not function as an effective channel agonist given that cytosolic levels of ATP in cardiac cells (5−10 mM) (*4*) far exceed cellular concentrations of SAM (60−90 μM) (*5*). Our data suggest SAM acts via an indirect yet undetermined mechanism to reduce channel conductance; however, the functional implication of substates in RyRs is unknown; therefore the role of SAM as a physiological regulator of RyR2 is uncertain.

Considering the present data, multiple mechanisms are suggested to account for the effects of SAM on RyR2 activation and conductance. We propose SAM activation of RyR2 results from a direct interaction with the channel, most likely binding the adenine nucleotide site(s). The observed effect of SAM on RyR2 conductance presumably occurs via an indirect mechanism in which SAM reduces channel conductance by causing a conformational change in the RyR2 protein. Such an effect may result from the SAM-induced loss of an undetermined RyR2 accessory protein. Determining the mechanism by which SAM causes RyR2 substates will further our understanding of the biophysical properties of RyR2 regulation.

REFERENCES

1. Bers, D. M. (2004) Macromolecular complexes regulating cardiac ryanodine receptor function. *J. Mol. Cell. Cardiol. 37*, 417–429.
2. Meissner, G. (1994) Ryanodine receptor/Ca^{2+} release channels and their regulation by endogenous effectors. *Annu. Rev. Physiol. 56*, 485–508.
3. Meissner, G. (1984) Adenine nucleotide stimulation of Ca^{2+}-induced Ca^{2+} release in sarcoplasmic reticulum. *J. Biol. Chem. 259*, 2365–2374.
4. Laver, D. R. (2006) Regulation of ryanodine receptors from skeletal and cardiac muscle during rest and excitation. *Clin. Exp. Pharmacol. Physiol. 33*, 1107–1113.
5. Hoffman, D. R., Cornatzer, W. E., and Duerre, J. A. (1979) Relationship between tissue levels of S-adenosylmethionine, S-adenylhomocysteine, and transmethylation reactions. *Can. J. Biochem. 57*, 56–65.
6. Bedford, M. T., and Richard, S. (2005) Arginine methylation an emerging regulator of protein function. *Mol. Cell 18*, 263–272.
7. Boisvert, F. M., Chenard, C. A., and Richard, S. (2005) Protein interfaces in signaling regulated by arginine methylation. *Sci. STKE 2005,* re2.
8. Gupta, M. P., Panagia, V., and Dhalla, N. S. (1988) Phospholipid N-methylation-dependent alterations of cardiac contractile function by L-methionine. *J. Pharmacol. Exp. Ther. 245*, 664–672.

9. Panagia, V., Gupta, M. P., Ganguly, P. K., and Dhalla, N. S. (1988) Methionine-induced positive inotropic effect in rat heart: possible role of phospholipid N-methylation. *Circ. Res. 62*, 51–55.
10. Chen, Y. F., Zhang, A. Y., Zou, A. P., Campbell, W. B., and Li, P. L. (2004) Protein methylation activates reconstituted ryanodine receptor-Ca release channels from coronary artery myocytes. *J. Vasc. Res. 41*, 229–240.
11. Ledbetter, M. W., Preiner, J. K., Louis, C. F., and Mickelson, J. R. (1994) Tissue distribution of ryanodine receptor isoforms and alleles determined by reverse transcription polymerase chain reaction. *J. Biol. Chem. 269*, 31544–31551.
12. Neylon, C. B., Richards, S. M., Larsen, M. A., Agrotis, A., and Bobik, A. (1995) Multiple types of ryanodine receptor/Ca^{2+} release channels are expressed in vascular smooth muscle. *Biochem. Biophys. Res. Commun. 215*, 814–821.
13. Jiang, D., Xiao, B., Li, X., and Chen, S. R. (2003) Smooth muscle tissues express a major dominant negative splice variant of the type 3 Ca^{2+} release channel (ryanodine receptor). *J. Biol. Chem. 278*, 4763–4769.
14. Kampfer, A. J., and Balog, E. M. (2008) S-Adenosyl-L-methionine activates the cardiac ryanodine receptor. *Biochem. Biophys. Res. Commun. 371*, 606–609.
15. Fruen, B. R., Kane, P. K., Mickelson, J. R., and Louis, C. F. (1996) Chloride-dependent sarcoplasmic reticulum Ca^{2+} release correlates with increased Ca^{2+} activation of ryanodine receptors. *Biophys. J. 71*, 2522–2530.
16. Sitsapesan, R., and Williams, A. J. (1990) Mechanisms of caffeine activation of single calcium-release channels of sheep cardiac sarcoplasmic reticulum. *J. Physiol. 423*, 425–439.
17. Ahern, G. P., Junankar, P. R., and Dulhunty, A. F. (1997) Subconductance states in single-channel activity of skeletal muscle ryanodine receptors after removal of FKBP12. *Biophys. J. 72*, 146–162.
18. Laemmli, U. K. (1970) Cleavage of structural proteins during the assembly of the head of bacteriophage T4. *Nature 227*, 680–685.
19. Chu, A., Diaz-Munoz, M., Hawkes, M. J., Brush, K., and Hamilton, S. L. (1990) Ryanodine as a probe for the functional state of the skeletal muscle sarcoplasmic reticulum calcium release channel. *Mol. Pharmacol. 37*, 735–741.
20. Meissner, G., and el-Hashem, A. (1992) Ryanodine as a functional probe of the skeletal muscle sarcoplasmic reticulum Ca^{2+} release channel. *Mol. Cell. Biochem. 114*, 119–123.
21. Brooks, S. P., and Storey, K. B. (1992) Bound and determined: a computer program for making buffers of defined ion concentrations. *Anal. Biochem. 201*, 119–126.
22. Eloranta, T. O., and Raina, A. M. (1977) S-adenosylmethionine metabolism and its relation to polyamine synthesis in rat liver. Effect of nutritional state, adrenal function, some drugs and partial hepatectomy. *Biochem. J. 168*, 179–185.
23. Chan, W. M., Welch, W., and Sitsapesan, R. (2003) Structural characteristics that govern binding to, and modulation through, the cardiac ryanodine receptor nucleotide binding site. *Mol. Pharmacol. 63*, 174–182.
24. Sitsapesan, R., and Williams, A. J. (1994) Gating of the native and purified cardiac SR Ca^{2+}-release channel with monovalent cations as permeant species. *Biophys. J. 67*, 1484–1494.
25. Laver, D. R., Lenz, G. K., and Lamb, G. D. (2001) Regulation of the calcium release channel from rabbit skeletal muscle by the nucleotides ATP, AMP, IMP and adenosine. *J. Physiol. 537*, 763–778.
26. McManus, O. B., and Magleby, K. L. (1991) Accounting for the Ca^{2+}-dependent kinetics of single large-conductance Ca^{2+}-activated K^+ channels in rat skeletal muscle. *J. Physiol. 443*, 739–777.
27. Kermode, H., Williams, A. J., and Sitsapesan, R. (1998) The interactions of ATP, ADP, and inorganic phosphate with the sheep cardiac ryanodine receptor. *Biophys. J. 74*, 1296–1304.
28. Timerman, A. P., Ogunbumni, E., Freund, E., Wiederrecht, G., Marks, A. R., and Fleischer, S. (1993) The calcium release channel of sarcoplasmic reticulum is modulated by FK-506-binding protein. Dissociation and reconstitution of FKBP-12 to the calcium release channel of skeletal muscle sarcoplasmic reticulum. *J. Biol. Chem. 268*, 22992–22999.
29. Pessah, I. N., Stambuk, R. A., and Casida, J. E. (1987) Ca^{2+}-activated ryanodine binding: mechanisms of sensitivity and intensity modulation by Mg^{2+}, caffeine, and adenine nucleotides. *Mol. Pharmacol. 31*, 232–238.
30. Zucchi, R., and Ronca-Testoni, S. (1997) The sarcoplasmic reticulum Ca^{2+} channel/ryanodine receptor: modulation by endogenous effectors, drugs and disease states. *Pharmacol. Rev. 49*, 1–51.
31. Ahern, G. P., Junankar, P. R., and Dulhunty, A. F. (1994) Single channel activity of the ryanodine receptor calcium release channel is modulated by FK-506. *FEBS Lett. 352*, 369–374.
32. Xiao, J., Tian, X., Jones, P. P., Bolstad, J., Kong, H., Wang, R., Zhang, L., Duff, H. J., Gillis, A. M., Fleischer, S., Kotlikoff, M., Copello, J. A., and Chen, S. R. (2007) Removal of FKBP12.6 does not alter the conductance and activation of the cardiac ryanodine receptor or the susceptibility to stress-induced ventricular arrhythmias. *J. Biol. Chem. 282*, 34828–34838.
33. Marx, S. O., Reiken, S., Hisamatsu, Y., Jayaraman, T., Burkhoff, D., Rosemblit, N., and Marks, A. R. (2000) PKA phosphorylation dissociates FKBP12.6 from the calcium release channel (ryanodine receptor): defective regulation in failing hearts. *Cell 101*, 365–376.
34. Ching, L. L., Williams, A. J., and Sitsapesan, R. (1999) AMP is a partial agonist at the sheep cardiac ryanodine receptor. *Br. J. Pharmacol. 127*, 161–171.
35. Chan, W. M., Welch, W., and Sitsapesan, R. (2000) Structural factors that determine the ability of adenosine and related compounds to activate the cardiac ryanodine receptor. *Br. J. Pharmacol. 130*, 1618–1626.
36. Ganguly, P. K., Panagia, V., Okumura, K., and Dhalla, N. S. (1985) Activation of Ca^{2+}-stimulated ATPase by phospholipid N-methylation in cardiac sarcoplasmic reticulum. *Biochem. Biophys. Res. Commun. 130*, 472–478.